All-optical 40Gb/s Cross-Wavelength Transferred Clock Recovery For 3R Wavelength Conversion Using a Traveling-wave Electroabsorption Modulator-Based Resonant Cavity

Zhaoyang Hu, Bin Liu, Xuejin Yan, John E. Bowers, and Daniel J. Blumenthal
Department of Electrical & Computer Engineering, University of California, Santa Barbara, CA 93106
Tel: (805) 893-5614, Fax: (805) 893-5707, E-mail:huby@ece.ucsb.edu

Abstract: An all-optical, compact clock recovery is demonstrated by utilizing filtered and actively amplified photocurrent in a traveling-wave electroabsorption modulator. 40GHz optical clock was recovered from 40Gb/s OTDM and transferred to new clock wavelength.

OCIS codes: (060.2330) Fiber optics communications, (070.4560) Optical data processing

1. Introduction

3R regeneration (retiming, reshaping and amplification) is considered a key-function for the future high-speed optical networks [1]. In 3R optical regenerative wavelength converters, the optical clock recovery (OCR) is performed first and the recovered clock pulses are launched through a wavelength converter with the data signal allowing the signal to be reshaped and re-timed as it is converted to a new wavelength. In previous approaches, the data signal was tapped from the input, photodetected, the clock recovered with a phase-locked loop (PLL) or a high Q filter and the data was optoelectronically regenerated [2][3].

In this paper, we demonstrate an all-optical clock recovery (OCR) hybrid integrated circuit that simultaneously provides optical recovery clock and the original data on two different wavelengths as shown in Fig.1(a). The modulation effect of the recovered electrical clock could suppress the inter-channel cross-talks in the output optical data signal from the OCR [4]. The OCR is designed so that the data signal (λ_1) input to the OCR can be input to a subsequent 3R wavelength converter with the optical recovery clock (λ_2) to achieve the 3R conversion to λ_2. The shadow part in Fig.1(a) represents the result of this paper, a hybrid integration resonant cavity OCR using a traveling-wave electroabsorption modulator (TW-EAM), a Q bandpass filter and a microwave monolithic IC (MMIC) amplifier interconnected by several coplanar waveguide (CPW) lines. Details of the TW-EAM have been previously reported in [5]. The TW-EAM simultaneously detects the clock component as a photodetector and generates the optical clock as a pulse generator. Hybrid integration allows the loop length to be minimized and reduce the capture time for synchronization to the data stream. The resonant cavity with several millimeter length indicates nanosecond-order capture time. Analytical modeling shows that the photocurrent generation from nonlinear electroabsorption process of the TW-EAM provides the loop phase tuning mechanism through adjusting the reverse bias of the TW-EAM.

2. Principle of Operation

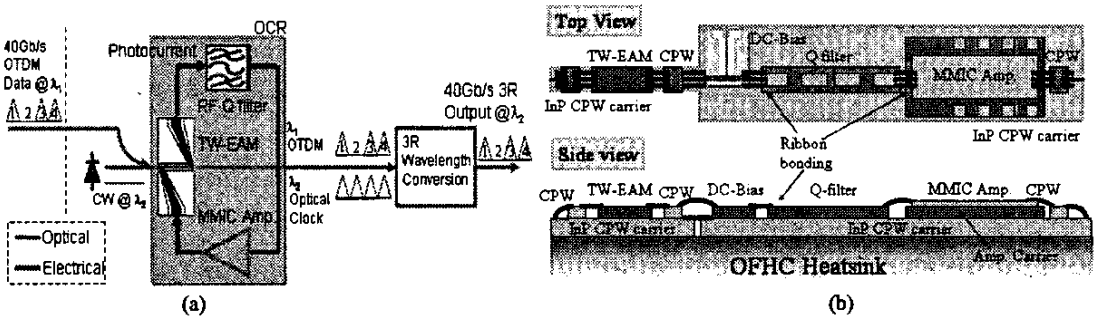

Fig. 1 (a) 3R architecture using the resonant cavity OCR (b) Hybrid integration configuration of the resonant cavity OCR

Fig. 1 (b) shows the configuration of the hybrid integration resonant cavity OCR including the TW-EAM, a DC-bias circuit, a coplanar waveguide high Q filter and a 40GHz narrowband MMIC amplifier. Two InP-

based CPW carriers underneath are fabricated to mount the components and contain the interconnections for the feedback loop. Although a phase shifter was not employed in the loop, the loop phase tuning can be obtained through adjusting the reverse bias voltage of the TW-EAM due to the photocurrent $I_{ph} = \eta_m(V)(p_0 + p\cos\omega_{in}t)$ generating from nonlinear electroabsorption process, where $p_0 + p\cos\omega_{in}t$ is the input optical power and $\eta_m(V)$ is the TW-EAM's detection responsivity. The photocurrent is filtered out at ω_{in} frequency component by the Q bandpass filter, amplified by the RF amplifier, and fed back to the lower electrical port of the TW-EAM as $V'(t) = V_1\cos[\omega_{in}(t+\tau)+\phi_1]$, where

$$V_1 = g\sqrt{\left[\begin{array}{l} Rp(A + B_1V_b + B_2V_b^2 + \frac{1}{2}B_2V_m^2) + \\ V_m(Rp_0B_1 + 2Rp_0B_2V_b + \alpha)\cos\phi + \frac{1}{4}RpB_2V_m^2\cos 2\phi \end{array}\right]^2 + \left[\begin{array}{l} V_m(Rp_0B_1 + 2Rp_0B_2V_b + \alpha)\sin\phi \\ + \frac{1}{4}RpB_2V_m^2\sin 2\phi \end{array}\right]^2} \quad (1)$$

$$\phi_1 = \arctan\left(\frac{V_m(Rp_0B_1 + 2Rp_0B_2V_b + \alpha)\sin\phi + \frac{1}{4}RpB_2V_m^2\sin 2\phi}{p(A + B_1V_b + B_2V_b^2 + \frac{1}{2}B_2V_m^2) + \frac{1}{4}RpB_2V_m^2\cos 2\phi + V_m(Rp_0B_1 + 2Rp_0B_2V_b + \alpha)\cos\phi}\right) \quad (2)$$

where V_b is the reverse bias of the TW-EAM, the oscillation signal in the loop is $V_m\cos(\omega_{in}t+\phi)$, ϕ is the initial phase of the RF signal relative to the optical signal, $\eta_m(V)$ is considered as second-order polynomial fitting $A + B_1V + B_2V^2$ basing on the measured relationship between photocurrent and reverse bias, α is the insertion loss of the TW-EAM, g is the net loop voltage gain including the loss in the loop and R is the TW-EAM's load impedance. The injection locked oscillation conditions should satisfy amplitude of $V_1 = V_m$ and phase $\phi_1 + \omega_{in}\tau = \phi + 2N\pi$, where τ is the loop delay and N is an integer [6]. From Eqn. (2), we can observe that tuning the reverse bias can shift the phase in the loop.

3. Resonant cavity OCR fabrication

The TW-EAM used in the OCR has total extinction ratio of above 30dB for the transverse magnetic (TM) mode. Its 3dB bandwidth as a photodetector is 12 GHz but the roll-off is slow and extends out to very high frequencies [7]. At 6dBm input power of 40Gb/s OTDM signal, the electrical 40GHz tone from TW-EAM's photocurrent is –40 dBm shown in Fig. 2(a).

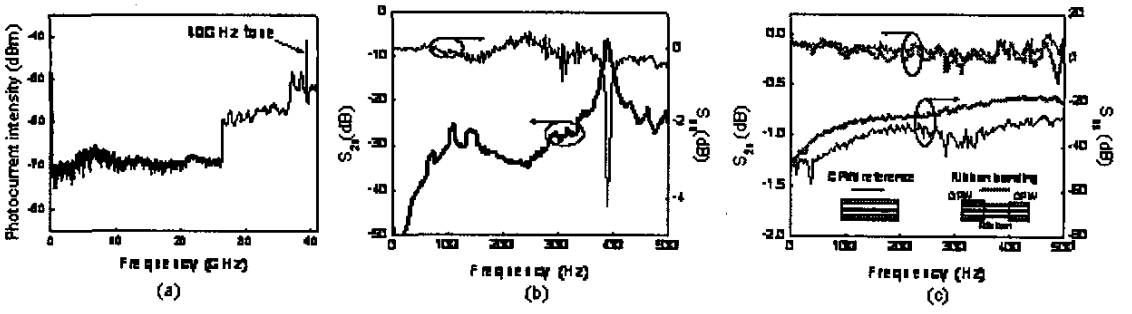

Fig. 2 (a) RF spectrum of TW-EAM photocurrent at 5dBm 40Gb/s OTDM signal (b) S-parameter of 40GHz coplanar Q bandpass filter (c) S-parameter of the CPW lines w/o ribbon bonding

The CPW lines, carriers and 40GHz coplanar Q bandpass filters are designed to have 50Ω characteristic impedance. All CPW lines, carriers and Q filters were fabricated on the semi-insulation InP substrate with a fixed ground-to-ground spacing of 35μm and the inner conductor width of 50μm, respectively. Ti/Au (20nm/1.2μm) films were deposited on the semi-insulation InP substrate by E-Beam, and then metal liftoff to transfer the patterns. The Q filters are realized by creating capacitively coupled resonant section in the inner conductor [8]. As shown in Fig. 2(b), its Q factor is about 50, sideband suppression ratio is above 20dB and the insertion loss is about 6dB. 50μm wide gold ribbons were employed and the loss due to ribbon bonding was negligibly low compared with the reference CPW lines, which is shown in Fig.2(c). A 36GHz-43GHz MMIC amplifier chip (XP1004, Mimix

Broadband Co.) with 26dB gain was soldered on the carrier for compensating the loop loss mainly came from the insertion loss of the TW-EAM and Q filter. The whole loop length is about 18mm coarsely adjusted for around 40GHz operation.

4. OCR experimental results

The experimental setup is shown in Fig.3(a) and the OCR (inner picture) was bonded on a fan-out submount so that the gate and drain bias voltages of the MMIC amplifier can be applied without DC probes. A 10GHz gain switched DBR laser was used to generate pulses at 1554nm (λ_1) and modulated with 2^{31}-1 PRBS pattern and then multiplexed to 40Gb/s optically. The CW light input was 6dBm at 1558 nm. A 2.4 nm optical band-pass filter was used to separate the 40Gb/s signal at 1554nm and the 40GHz optical clock at 1558nm. A GSG RF probe and a bias-tee were used to provide the reverse bias for the TW-EAM and allow simultaneous extraction of the electrical clock from the OCR.

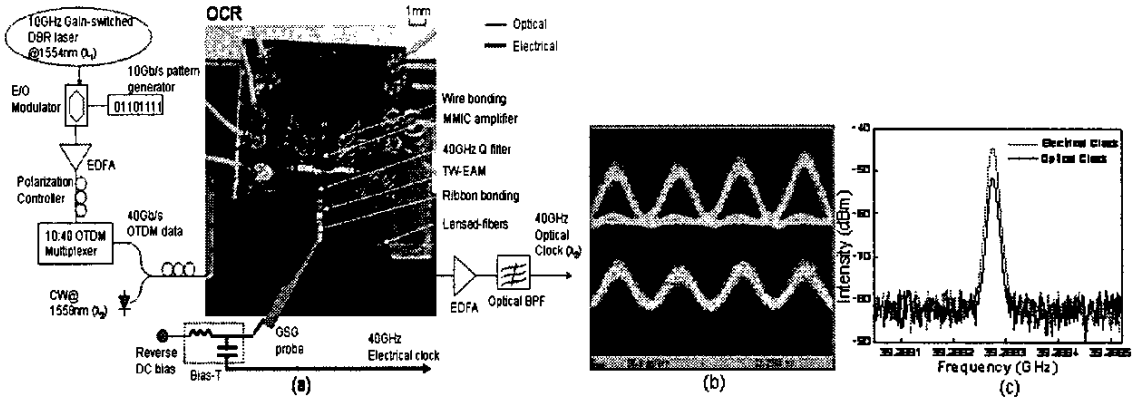

Fig. 3 (a) Measurement setup (b) ~40GHz optical recovery clock (lower) and input ~40Gb/s data eye diagram (c) RF spectra of the optical and electrical recovery clock (RBW: 10kHz, Span: 500kHz)

When around 40Gb/s OTDM signal inputs the OCR, both the clock component of 39.28828GHz and the neighbour free-running mode of 39.28839GHz exist in the loop. The free-running frequency of the OCR was fine-tuned close to clock frequency through adjusting the bias voltage to ~3.45V and immediately it was phase locked at clock frequency. The recovered optical clock detected at the new wavelength is shown in the lower part of Fig.3(b) and its RF spectrum in Fig.3(c). The absolute root-mean-square timing jitter of the optical and electrical clock is about 11ps, which is obtained by integrating the single side-band noise from their RF spectra.

5. Summary and Conclusion

Compact all-optical 40Gb/s resonant cavity OCR based on a TW-EAM was demonstrated. Both 40GHz optical and electrical recovery clock were simultaneously demonstrated. These results show that the hybrid integrated resonant cavity OCR works for optical and electrical clock recovery at 40Gb/s line rate. The low signal-noise-ratio of the recovery clock could be attributed to weak modulation of the TW-EAM which will be improved in the future. The whole structure is compact and potentially monolithic integration. The authors gratefully thank Drs. Lavanya Rau, Hsu-Feng Chou, Suresh Rangarajan, Vikrant Lal and Yi-Jen Chiu's helps and would like to acknowledge funding for this project under KDDI under grant 442530-59406 and a State of California UC Discovery grant 597095-19929.

References

[1] K.E. Stubkjaer, IEEE J. Selected Topics in Quantum Electronics, pp. 1428-1435, 2000.
[2] O. Leclerc, et.al., CFD14, CLEO 2000.
[3] D.T.K. Tong, et. al., vol. 36, pp. 1951-1952, Electronics Letters, 2000.
[4] K. Nishimura, et.al., pp. 286-287, ECOC 2001.
[5] Y.-J. Chiu et al., IEEE Photon. Technol. Lett., vol. 14, pp. 792-794, 2002.
[6] L. Huo, et. al., IEEE Photon. Technol. Lett., vol. 15, pp.981-983, 2003.
[7] H.-F. Chou, et. al.,pp.776-777, ECOC 2003.
[8] D.F. Williams, et. al., IEEE Trans. on Microwave Theory and Techniques, vol. MTT-31, pp. 558-566, 1983.